Supporting Information for

Highly Efficient Amorphous Zn_2SnO_4 Electron Selective Layers Yielding over 20% Efficiency in $FAMAPbI_3$-based Planar Solar Cells

Kyungeun Jung,[a,b] *Jeongwon Lee,*[b] *Chan Im,*[a] *Junghwan Do,*[a] *Joosun Kim,*[c] *Weon-Sik Chae,*[d] *Man-Jong Lee*[a,b,*]

[a] Department of Chemistry, Konkuk University, Seoul 143-701, Republic of Korea

[b] Department of Advanced Technology Fusion, Konkuk University, Seoul 143-701, Republic of Korea

[c] High Temperature Energy Materials Research Center, Korea Institute of Science and Technology, Seoul 136-791, Republic of Korea

[d] Analysis Research Division, Daegu Center, Korea Basic Science Institute, Daegu 702-701, Republic of Korea

Corresponding Author

* *E-mail: leemtx@konkuk.ac.kr (M.-J Lee)*

EXPERIMENTAL

Synthesis of am-ZTO films

Am-ZTO films, working as an electron selective layer (ESL), are synthesized by a simple solution process using zinc acetate (Sigma-Aldrich) and tin acetate (Sigma-Aldrich). Fluorine-doped tin oxide (FTO)-coated glass (Pilkington, Tec-8) were patterned using Zn powder and diluted HCl solution followed by cleaning subsequently in diluted hellmanex, acetone, ethanol, and deionized water. Then, 2-methoxyethanol (Sigma-Aldrich) solutions are prepared by dissolving zinc acetate and tin acetate while maintaining the 2:1 molar ratio of zinc to tin, where ethanolamine (Sigma-Aldrich) was added as a stabilizing agent to improve the solubulity of precursor salts. The precursor solutions having the various source concentations from 0.15 M to 1.05 M were spin coated on the top of FTO glasses for 30s at 3000 rpm followed by drying at 150 °C for 5 m. Finally, ZTO coated FTO glasses are annealed at 500 °C for 1 h in an air atmosphere. By varying concentrations, the thickness of am-ZTO films was optimized. To make 80 nm blocking TiO_2 layer, working as an electron transfer layer (ETL), was prepared by the dynamic spin-coating of 0.2 M titanium diisopropoxide bis(acetylacetonate) solution in 1-butanol (Sigma-Aldrich) at 3000 rpm for 30 s. After drying at 100 □ for 5m, it was sintered at 500 □ for 30 m. To form a compact TiO_2, the sintered layer was treated by 20 mM $TiCl_4$ (WACO) solution at 70 □ for 10 m and then sintered at 500 □ for 30 m.

Synthesis of planar heterojunction PSCs

The $FA_xMA_{1-x}PbI_3$ perovskite absorber layer was fabricated by a two-step spin-coating procedure on the prepared substrates. Following the report of Li et al. [1], the selected concentration of FAI-MAI mixed perovskite precursor solution was prepared by dissolving 20

mg $MAPbI_3$ (MAI, Dyesol Korea) and 25 mg $FAPbI_3$ (FAI, Dyesol Korea) in 1 mL isopropyl alcohol (IPA). First, the 150 mg of PbI_2 (anhydrous, 99.9 %, TCI) in the mixed solvent of 220 μL dimethylformamide (DMF, Sigma-Aldrich) and 20 μL dimethyl sulfoxide (DMSO, Sigma Aldrich) were magnetically stirred for 24 h and the mixture solution was then coated on the ESL layer by the dynamic spin coating method at 3000 rpm for 30 s. After drying at 120 °C for 5 m, the mixed FAI-MAI solution of 50 μL with a constant concentration was continuously dropped on the as-prepared PbI_2 substrates during spin coating at 5000 rpm for 30 s and annealed at 150 °C for 10 m. In this process, no solvent was added, meaning that no additional solvent washing process was required. A hole transfer layer (HTL) was then coated via spin coating with the 20 μl of spiro-MeOTAD solution, which was consisted of 80 mg spiro-MeOTAD (1-material), 28.5 μl of 4-tert-butyl pyridine and 17.5 μl of lithium bis(trifl uoromethanesulfonyl)imide (Li-TFSI) solution (520 mg Li-TSFI in 1 ml acetonitrile (Sigma–Aldrich) in 1ml of chlorobenzene (Sigma–Aldrich), was spin-coated on the perovskite layer at 3000 rpm for 30 sec.

Characterizations

The crystal structure of perovskites was determined using X-ray diffraction (XRD, Rigaku Model SmartLab) with CuKα radiation. In addition, structural analysis was performed by glancing incidence X-ray diffraction (GIXRD) mode, using Cu Kα radiation at the incident angle of 0.2 to 1 ° to the specimen surface. Furthermore, Grazing-Incidence Small-Angle X-ray Scattering (GISAXS, Bruker D8 Discover) analyses were performed at the incident angle of 1 ° to confirm the amorphous structure of thin films. High-resolution Transmission Microscopy (HRTEM, Cs-Corrected, JEOL, JEM-ARM200F) measurements were also performed to identify

the crystal structure. The morphology of the synthesized films was also examined using a field-emission scanning electron microscope (FE-SEM, JSM-7500F, JEOL) with resolution at 15 kV. UV-Vis-near-infrared (NIR) transmittance and reflectance spectra were obtained using a UV-Vis-NIR spectrophotometer (Optizen POP) equipped with a diffuse reflectance accessory. The photovoltaic properties of the assembled PSCs were determined using a solar simulator (Polaronix K201, Mc-science, Korea) equipped with a 150-W xenon lamp and a Keithley 2401 source meter under AM 1.5 simulated sunlight with a power density of 100 mW/cm². All the measurements were performed by masking the cells with a metal aperture to define the active area of 0.09 cm² after the intensity calibration with an NREL-calibrated KG5 filtered Si reference cell. An incident photon-to-current conversion efficiency (IPCE) measurement system (HS Tech, Korea) was used to evaluate the external quantum efficiency (EQE). FLIM was measured using an inverted-type scanning confocal microscope (MicroTime 200, Picoquant, Germany) with a 100× (oil-immersion) objective. A single-mode pulsed diode laser (470 nm with ~30 ps pulse width, ~0.1 μW average power, and 0.5 MHz repetition rate) was used as an excitation source. A dichroic mirror (490 DCXR, AHF), a long-pass filter (HQ500lp, AHF), a 100 μm pinhole, a 700 nm long-pass filter, and a single photon avalanche diode (PDM series, MPD) were used to collect emissions from the samples. Time-correlated single-photon counting (TCSPC) technique was used to count fluorescence photons. FLIM images, consisting of 200 × 200 pixels, were recorded using the time-tagged time-resolved (TTTR) data acquisition method. The acquisition time of each pixel was 2 ms. Exponential fittings for the obtained fluorescence decays, which were extracted from the FLIM images, were performed using SymPhoTime-64 software by an exponential decay model $I(t) = \sum A_i e^{-t/\tau_i}$, where $I(t)$ is the time-dependent PL intensity, A is the amplitude, τ is the PL lifetime, and i is 3. Steady-state fluorescence spectrum

at a focal volume was measured for the samples by guiding the fluorescence signal to the external spectrometer (F-7000, Hitachi). UPS was measured by Axis Supra (Kratos, U.K.). The AFM was measured by XE-100 (Park system, Korea).

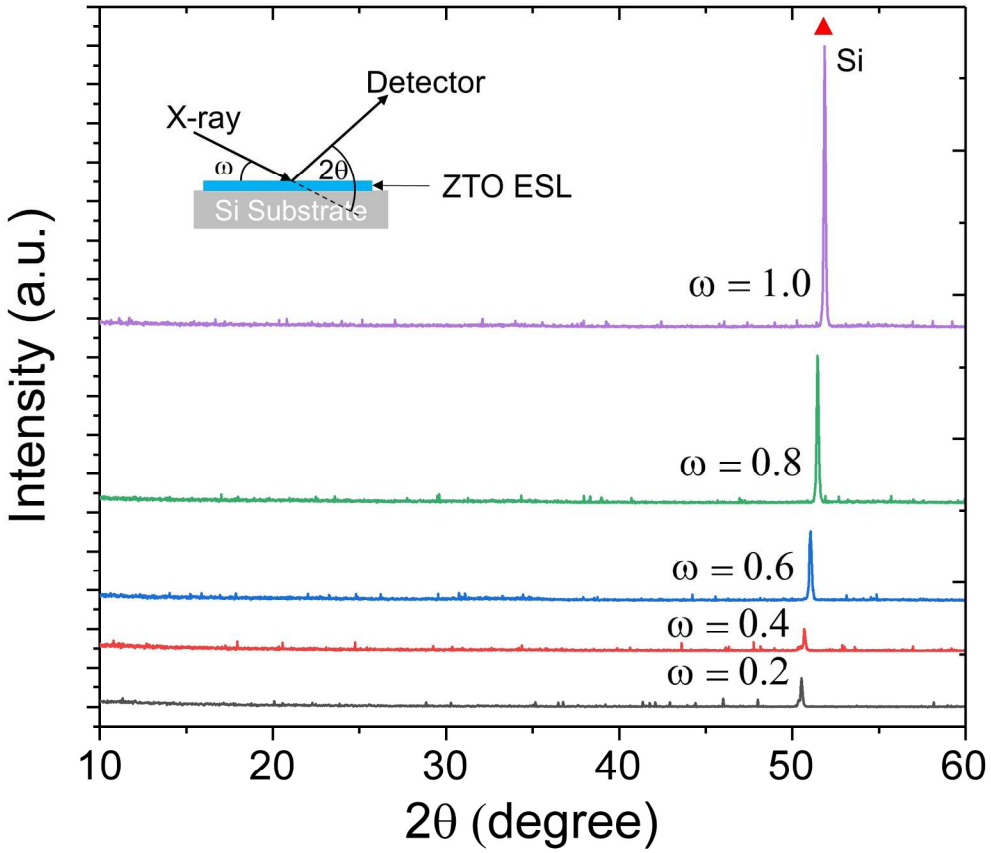

Figure S1. GI-XRD pattern of a ZTO ESL coated on the Si substrate. The incident angle to the specimen surface was changed from 0.2 to 1°.

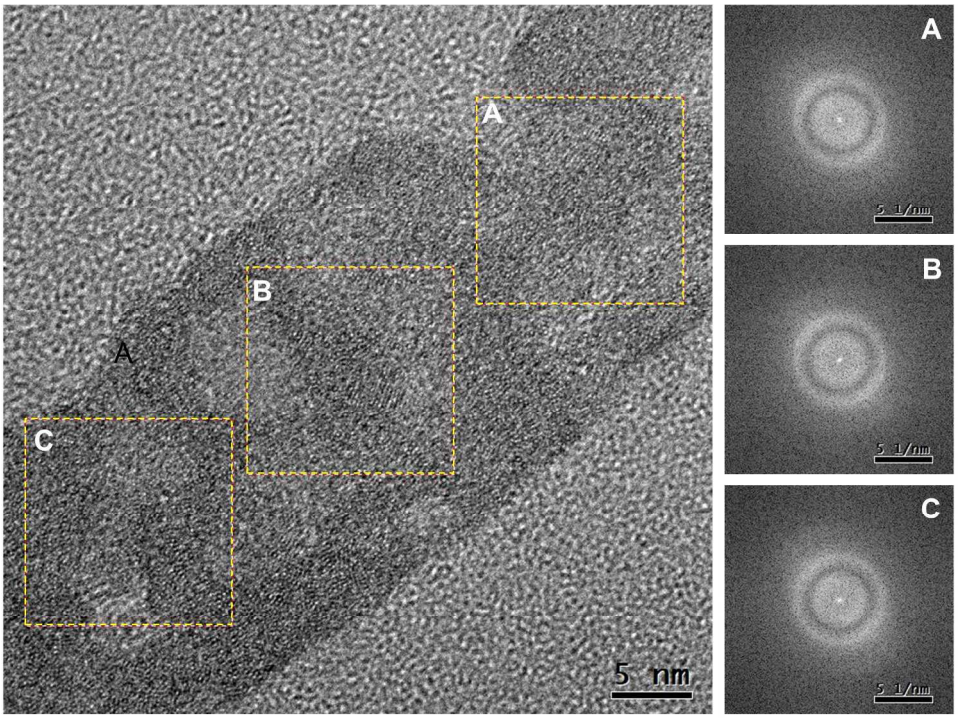

Figure S2. HRTEM image of a ZTO ESL film. Notice the entire ZTO areas show amorphous ring patterns obtained from the Fast Fourier Transformation of selected areas (A, B, and C).

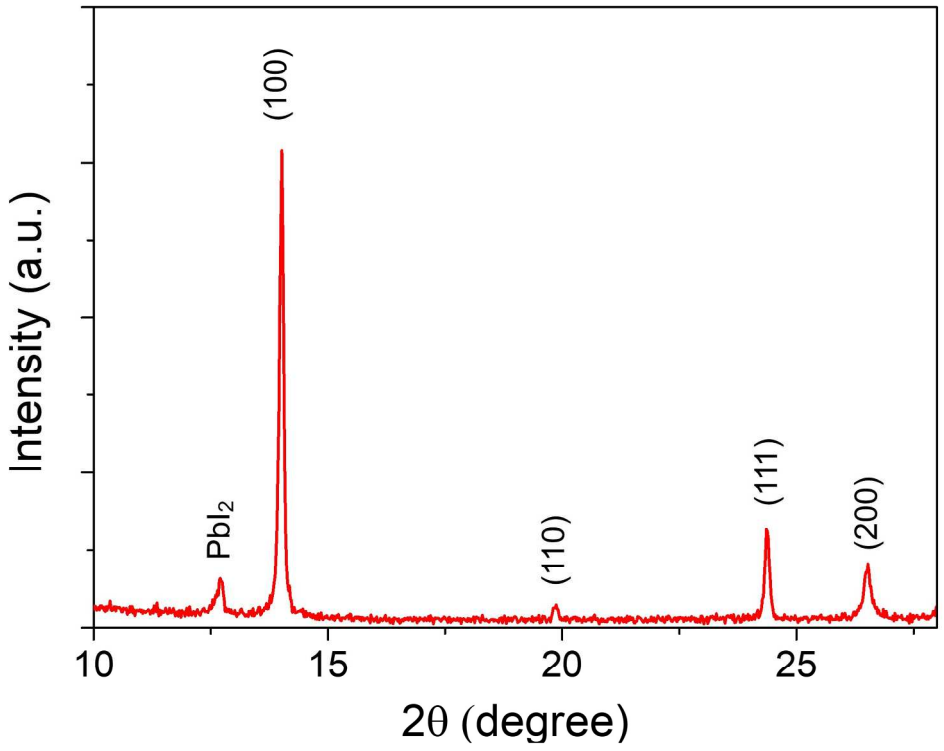

Figure S3. XRD pattern of a $FAMAPbI_3$ perovskite used in this study showing a single α-$FAPbI_3$ phase containing a small amount of PbI_2.

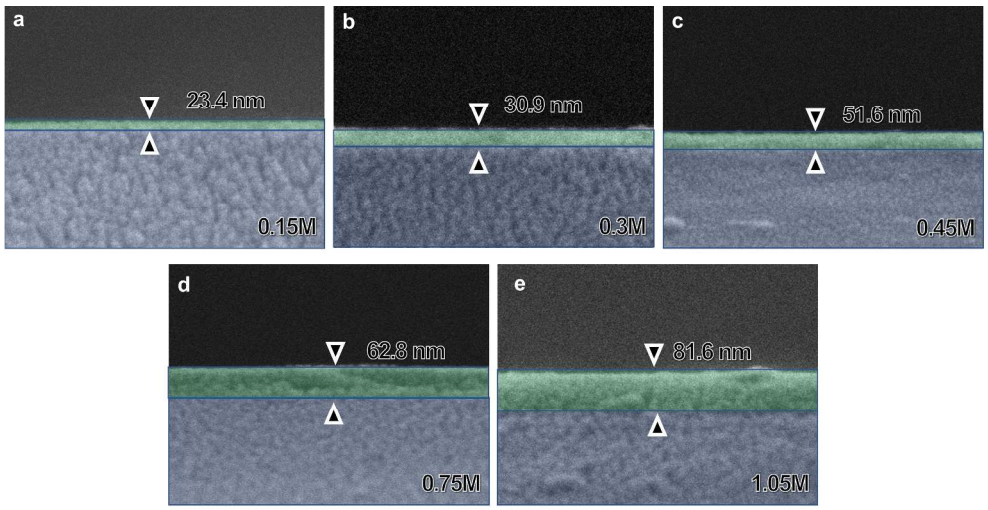

Figure S4. SEM images of am-ZTO coated FTO glasses showing the gradual increases in film thickness using the precursor concentrations of 0.15 M (a), 0.30 M (b), 0.45 M (c), 0.75 M (d), and 1.05 M (e), respectively.

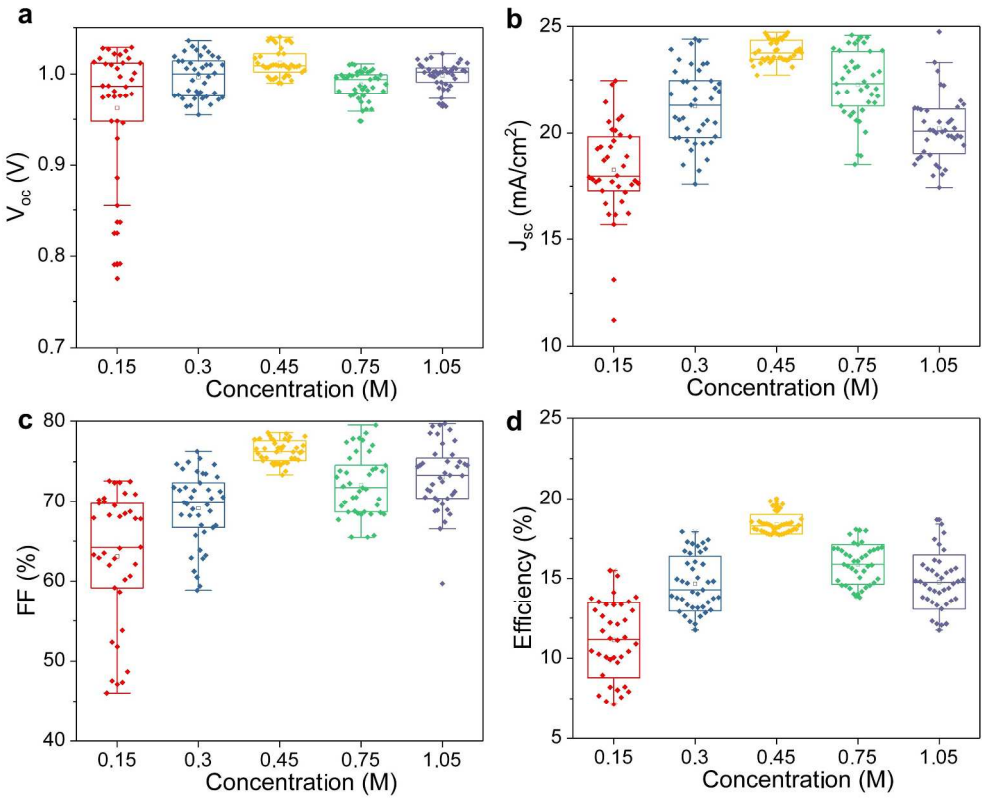

Figure S5. Variations in PV parameters (a–c) and PCEs (d) of PSCs based on am-ZTO synthesized at various precursor concentrations.

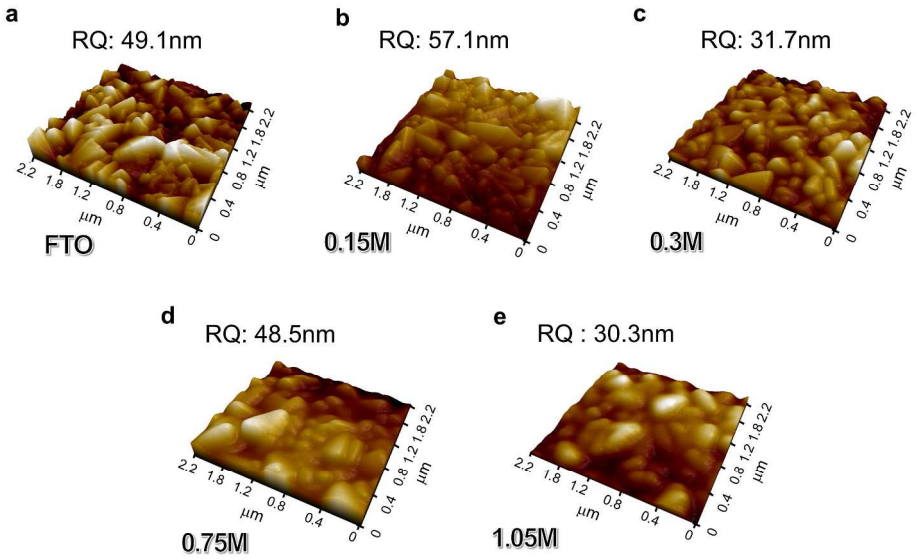

Figure S6. AFM images of (a) a bare FTO film and am-ZTO ESLs synthesized from the precursor concentrations of 0.15 M (b), 0.30 M (c), 0.75 M (d), and 1.05 M (e), respectively.

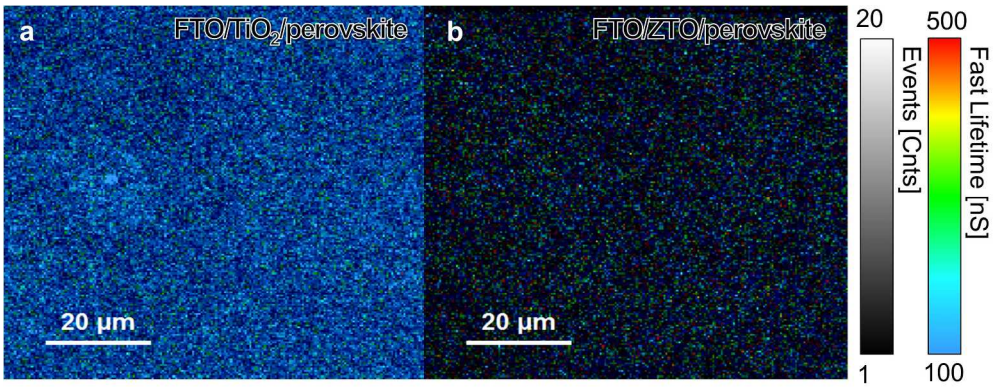

Figure S7. FLIMs of the structures of (a) FTO/TiO_2/perovskite (b) FTO/am-ZTO/perovskite showing the am-ZTO based structure has less PL events (darker) and faster lifetime (blue color) compared to the counterpart.

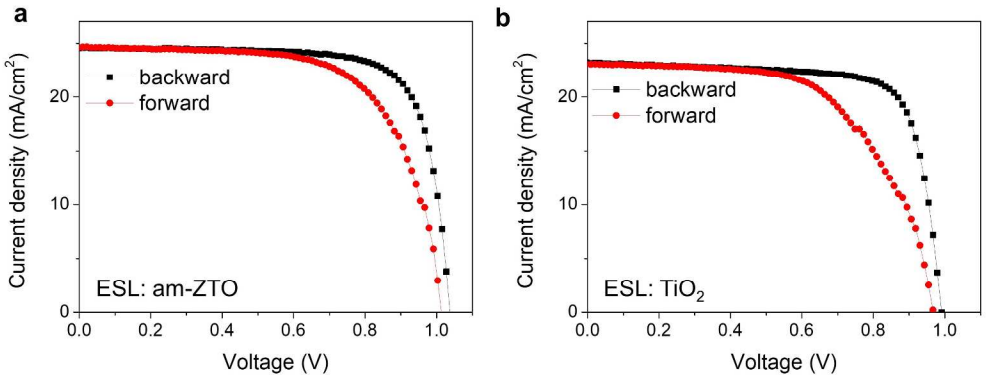

Figure S8. J-V curves of full devices (FTO/ESL/perovskite/MeOTAD/Au) based on (a) am-ZTO and (b) TiO_2 showing the hysteresis behavior.

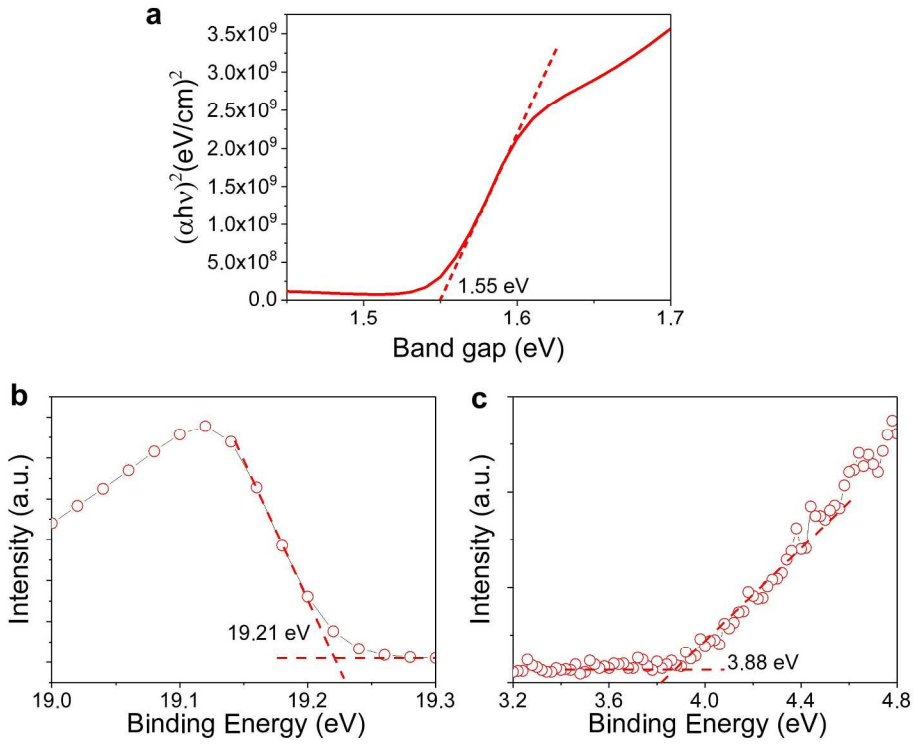

Figure S9. (a) Tauc plots ($(\alpha h\nu)^2$ vs. energy in *eV*) for the evaluation of E_g of perovskite films, (b,c) UPS spectra representing the $E_{cut\text{-}off}$ and $E_{F,edge}$ for perovskite films.

REFERENCES

1. Li, W.; Fan, J.; Li, J.; Niu, G.; Mai, Y.; Wang, L.; Wang, High Performance of Perovskite Solar Cells via Catalytic Treatment in Two-Step Process: The Case of Solvent Engineering, ACS Appl. Mater. Interfaces.**2016**, 8, 30107−30115.